Available online at www.sciencedirect.com

SCIENCE DIRECT®

ELSEVIER

Journal of Organometallic Chemistry 690 (2005) 1314–1323

Journal of Organo metallic Chemistry

www.elsevier.com/locate/jorganchem

Highly active new α-diimine nickel catalyst for the polymerization of α-olefins

Hua-Rong Liu [a,b], Pedro T. Gomes [a,*], Sandra I. Costa [a], M. Teresa Duarte [a],
R. Branquinho [a], Anabela C. Fernandes [a], James C.W. Chien [c],
R.P. Singh [d], Maria M. Marques [a,*]

[a] *Centro de Química Estrutural, Departamento de Engenharia Química, Instituto Superior Técnico, Av. Rovisco Pais 1, 1049-001 Lisboa, Portugal*
[b] *Department of Polymer Science and Engineering, University of Science and Technology of China, Hefei 230026, PR China*
[c] *Department of Polymer Science and Engineering, University of Massachusetts, Amherst, MA 01003, USA*
[d] *Division of Polymer Chemistry, National Chemical Laboratory, Pune 411 008, India*

Received 8 September 2004; accepted 29 November 2004

Abstract

A new silylated α-diimine ligand, bis[*N*,*N*′-(4-*tert*-butyl-diphenylsilyl-2,6-diisopropylphenyl)imino]acenaphthene **3**, and its corresponding Ni(II) complex, {bis[*N*,*N*′-(4-*tert*-butyl-diphenylsilyl-2,6-diisopropylphenyl)imino]acenaphthene}dibromonickel **4**, have been synthesized and characterized. The crystal structures of **3** and **4** were determined by X-ray crystallography. In the solid state, complex **4** is a dimer with two bridging Br ligands linking the two nickel centers, which have square pyramidal geometries. Complex **4**, activated either by diethylaluminum chloride (DEAC) or methylaluminoxane (MAO) produces very active catalyst systems for the polymerization of ethylene and moderately active for the polymerization of propylene. The activity values are in the order of magnitude of 10^7 g PE (mol Ni [E] h)$^{-1}$ for the polymerization of ethylene and of 10^5 g PP (mol Ni [P] h)$^{-1}$ for the polymerization of propylene. NMR analysis shows that branched polyethylenes (PE) are obtained at room or higher temperatures and almost linear PE is obtained at 0 °C with **4**/DEAC.

Keywords: α-Diimine nickel complex; Late transition-metal; Ethylene polymerization; Propylene polymerization

1. Introduction

There is a considerable interest in the development of new late transition metal catalysts for the polymerization of α-olefins since Brookhart and co-workers [1–3] discovered highly active α-diimine nickel and palladium catalysts which convert ethylene and α-olefins to high molar mass polymers with unique microstructures. These catalysts have been shown not only to be primarily useful for ethylene polymerization but also to promote co-polymerizations of olefins with polar monomers and functionalization of polyolefins [4–11]. In addition, the α-diimine ligands are well-known to stabilize organometallic complexes resulting in much more stable late transition metal catalysts compared with early transition metal catalysts [12]. This is beneficial to commercial applications and industrial production.

In this work, we report the synthesis and characterization of a new silylated α-diimine ligand, in which there is a –Si(^{t}Bu)Ph$_2$ substituent at the *para* position of the 2,6-dialkylaryl imine group, and its Ni dibromide complex. We also describe the catalytic behavior of this new complex towards ethylene and propylene polymeri-

---

[*] Corresponding authors. Tel.: +351 218419612/3; fax: +351 218414457/5.
E-mail addresses: pedro.t.gomes@ist.utl.pt (P.T. Gomes), pci011@mail.ist.utl.pt (M.M. Marques).

0022-328X/$ - see front matter © 2004 Elsevier B.V. All rights reserved.
doi:10.1016/j.jorganchem.2004.11.046

zation. One of the aims would be the modification of the ligand structure in order to change the electronic density at the metal center, thus inducing different activities, polymer microstructures or degrees of co-monomers incorporation.

2. Results and discussion

2.1. Syntheses and characterizations of ligand **3** and complex **4**

In order to synthesize the target silylated α-diimine ligand, the appropriate aniline **2** was first prepared by bromination of diisopropylaniline at position 4, yielding compound **1**, followed by substitution reaction with *tert*-butyldiphenylsilyl chloride. The reaction sequence leading to the synthesis of the novel compound **2** is depicted in Scheme 1.

In the bromination reaction, Oskam and co-workers [13] obtained 4-Br-2,6-$^{i}Pr_2$-$C_6H_2NH_2$ in 61% yield by adding Br_2 to a stirred slurry of 2,6-$^{i}Pr_2$–$C_6H_3NH_3Cl$ in glacial acetic acid. In the present work, a modification of this synthetic procedure was introduced since the ammonium salt was poorly soluble in glacial acetic acid. Instead, we have used methanol/glacial acetic acid (2:1(v/v)) as the reaction solvent, enabling the dissolution of the reagents and leading to an increased yield of compound **1** (79%) in relation to the literature [13].

Usually, the amine group of compound **1** should be protected before the substitution reaction of bromide in position 4 by the *tert*-butyldiphenylsilyl group. However, in this case, the amine hydrogens seem to be not very reactive due to steric hindrance of the bulky diisopropyl groups in both *ortho* positions. In addition, we have chosen the bulky *tert*-butyllithium to substitute the Br, further preventing the reaction of the amine with *tert*-butyldiphenylsilyl chloride in the next step. In fact, none of the hydrogen atoms in the amine were substituted by the *tert*-butyldiphenylsilyl group. Compound **2** is obtained in low yield (25%) due to the simultaneous formation of two unidentified by-products. Three distinct bands were obtained after separation by column chromatography, being the desired product **2** isolated from the middle fraction as white needles.

The new ligand **3** was prepared by condensation reaction of acenaphthenequinone with the silylated aniline **2** according to a literature procedure [14] (see Scheme 2). Recrystallization of the crude ligand from hot toluene afforded air stable orange crystals in 64% yield.

Complex **4** was prepared via two different procedures [14] (Scheme 2): (a) one-pot reaction of $NiBr_2$, acenaphthenequinone and 2,6-diisopropyl-4-*tert*-butyldiphenylsilyl-aniline **2** in glacial acetic acid, and (b) addition of the diimine ligand **3** to [$NiBr_2$(DME)] in CH_2Cl_2. It is obtained in good yields (61% and 87%, respectively) as a dark red-brown powder. Due to the geometry around the nickel atom, this α-diimine Ni(II) complex is paramagnetic and its ^{1}H NMR is not assignable. Elemental analysis of complex **4** fits the molecular structure obtained by X-ray structural studies. This compound is air stable but do require moisture-free solvents during

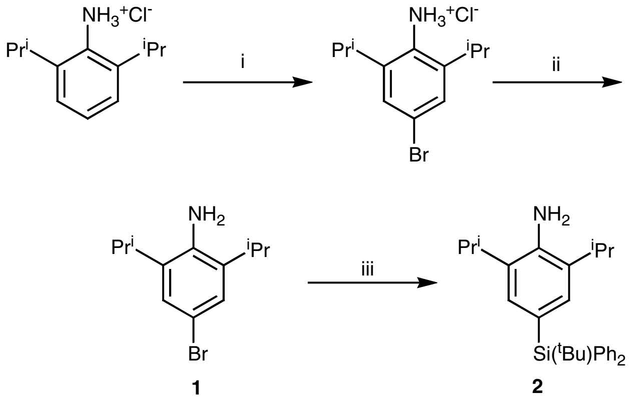

Scheme 1. Synthesis of compounds **1** and **2**. Reagents: (i) 2,6-di-i-propylaniline hydrochloride (1 equiv) in MeOH/CH_3COOH, Br_2 (1 equiv), room temperature, 2.5 h. (ii) NaOH in water/Et_2O, room temperature. (iii) Li^{t}Bu (3 equiv) in THF, −70 °C to room temperature, overnight, then $Ph_2(^tBu)SiCl$ (1 equiv), −20 °C to room temperature, overnight.

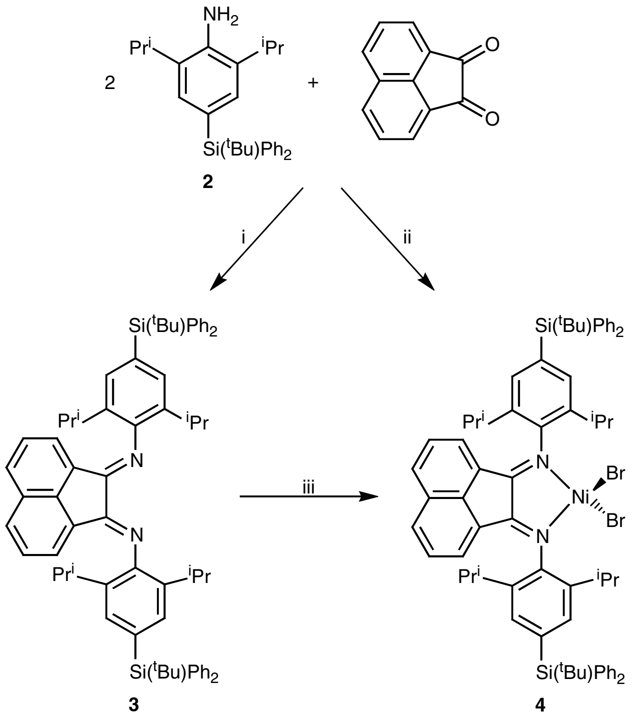

Scheme 2. Synthesis of compounds **3** and **4**: (i) in MeOH, formic acid (catalytic amount), room temperature, 3 days; (ii) in glacial acetic acid, reflux, 4 h, then anhydrous $NiBr_2$ (1 equiv), reflux, 16 h; (iii) [$NiBr_2$(DME)] (1 equiv), in CH_2Cl_2, room temperature, overnight.

handling. The use of glacial acetic acid does not interfere with the formation of the nickel complex, which suggests that it is acid-stable with respect to decomposition. In addition, the *tert*-butyldiphenylsilyl group is stable to hydrolysis. This highly polarizable substituent also confers increased solubility properties to the complex since, compared to its non-silylated analogue, it is fairly soluble in toluene.

Recrystallization of ligand **3**, by cooling a toluene solution overnight to −20 °C, gave crystals suitable for X-ray crystal structure determination. The molecular structure of **3** is shown in Fig. 1, and selected bond lengths and angles are presented in Table 1. The ligand exhibits a *pseudo* C_{2v} symmetry with different electron density distributions on both sides of the ligand, visible when comparing the C=N imine and the N–C_{aryl} bonds (respectively, 1.274(7), 1.308(7) Å) and 1.488(7), 1.367(8) Å). The relatively long C1–C11 bond distance, 1.536(7) Å, compared to the expected C_{sp^2}–C_{sp^2} single bond, 1.48 Å [15], is due to the constraints existing in the five membered ring. The bis(imino)acenaphthene skeleton is planar as shown by the torsion angles N1–C1–C11–N2 and C2–C1–C11–C10 of −1.8(7) and 0.1(7)°, respectively. This planarity is extended to the imine–aryl bonds, proved by the low values of the torsion angles C1–C11–N2–C41 and C11–C1–N1–C13 of 2.1(5) and 1.3(5)°. Both aryl rings, practically parallel to each other (dihedral angle of 2.3(2)°), are almost perpendicular to the bis(imino)acenaphthene plane (dihedral angles of 79.3(2) and 80.3(2)). Due to the overall stereochemical constraints of the molecule, the N atoms of the imine groups display short interactions with the hydrogen atoms of the isopropyl substituents of the phenyl rings, both above and below the plane of the molecule (C–H···N, interactions with H···N distances in the order of 2.412(4), 2.471(6), 2.496(6) and 2.532(4) Å). These structural features compare well with those found in the non-silylated analogue (*i*PPBIAN) [16] or in the *p*-tolyl derivative (*p*-Tol-BIAN) [17] and related compounds referred therein.

Table 1
Selected bond distances (Å) and angles (°) for ligand **3** and the corresponding nickel complex **4**

	3	4
N1–C1	1.274(7)	1.274(10)
N1–C13	1.488(7)	1.458(10)
N2–C11	1.308(7)	1.280(11)
N2–C41	1.367(8)	1.444(12)
C1–C11	1.536(7)	1.556(12)
C1–C2	1.490(7)	1.459(12)
C11–C10	1.491(7)	1.479(12)
C10–C12	1.423(10)	1.394(12)
C12–C2	1.403(9)	1.423(12)
Ni–Br1	–	2.412(2)
Ni–Br2	–	2.447(2)
Ni–Br2[a]	–	2.470(2)
Ni–N1	–	2.106(8)
Ni–N2	–	2.073(8)
Ni···Ni[a]	–	3.49(2)
C1–N1–C13	118.3(5)	118.6(9)
N1–C1–C11	118.4(5)	116.8(10)
C1–C11–N2	120.6(4)	116.4(9)
C11–N2–C41	119.1(5)	117.0(9)
N1–C13–C14	117.4(5)	121.8(10)
N1–C13–C18	118.2(5)	116.1(10)
N2–C41–C42	118.6(6)	122.2(11)
N2–C41–C46	121.8(6)	116.7(12)
N1–Ni–N2	–	80.5(3)
N2–Ni–Br1	–	96.8(2)
N1–Ni–Br1	–	96.5(2)
N2–Ni–Br2	–	158.0(2)
N1–Ni–Br2	–	91.5(2)
Br1–Ni–Br2	–	104.48(7)
N2–Ni–Br2[a]	–	90.8(3)
N1–Ni–Br2[a]	–	158.9(2)
Br1–Ni–Br2[a]	–	103.67(7)
Br2–Ni–Br2[a]	–	89.55(6)

[a] Symmetry transformation $1 - x, -y, -z + 1$.

Complex **4** was also characterized by X-ray crystallography. Crystals were grown by slow diffusion of hexane into a CH_2Cl_2 solution of **4**. The molecular structure is depicted in Fig. 2 with selected bond lengths and angles in Table 1. It shows a dimeric structure composed by two centrosymmetrically related monomeric moieties, where

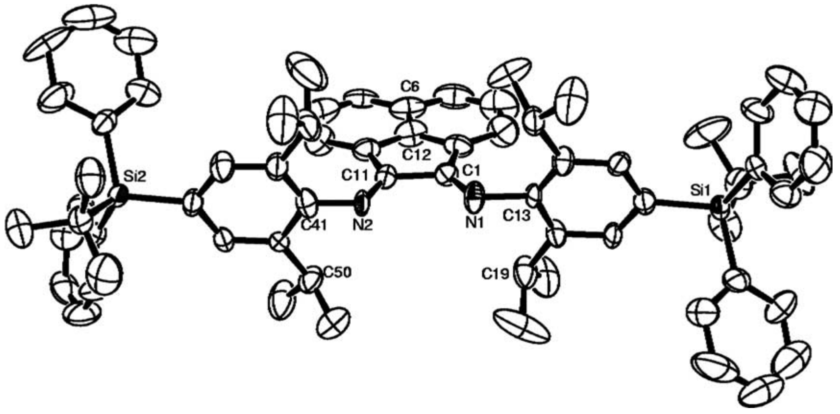

Fig. 1. Molecular structure of ligand **3**. Thermal ellipsoids are given with 40% probability level. Hydrogen atoms are omitted for clarity.

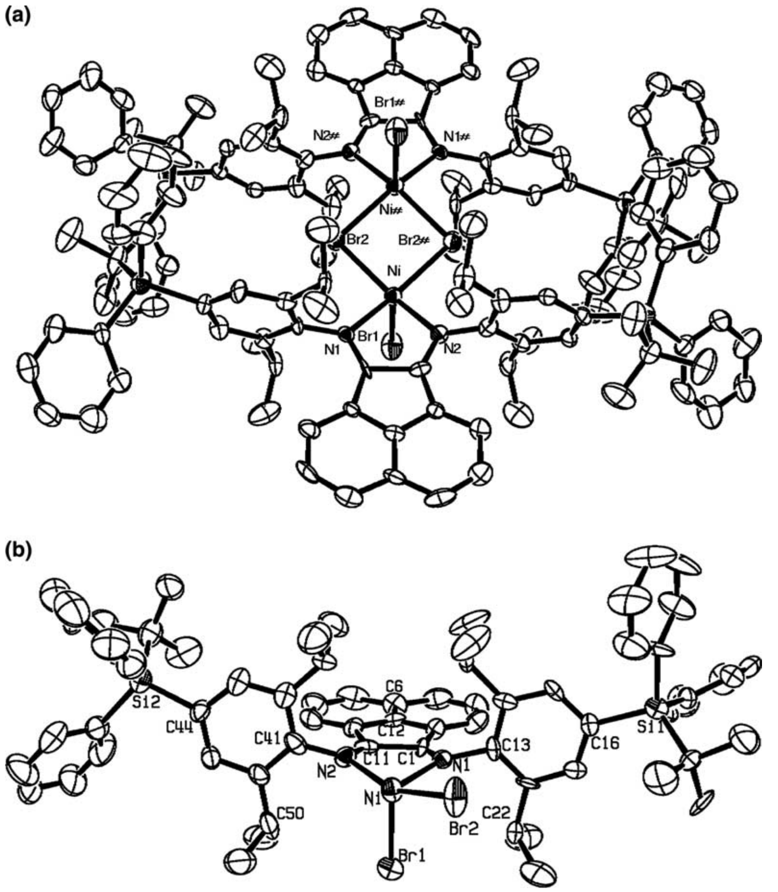

Fig. 2. Molecular structure of dimeric **4**. Thermal ellipsoids are given with 30% probability level. Hydrogen atoms are omitted for clarity. (a) Global view of the dimer. (b) View of one of moieties.

two bromine atoms (Br2) are bridging the two nickel centers (3.49(2) Å apart), which display a square pyramidal geometry. Each apical Br1 atom is 2.812(4) Å away from the basal square plane defined by the two nitrogen and the two bromine atoms, and the Ni atom stays at 0.414(3) Å from this plane. This dimeric structure is similar to those found for the non-silylated analogue [bis(*N*,*N*′-2,-6-diisopropylphenylimino)acenaphthene]dibromonickel ([NiBr$_2$(*i*PPBIAN)]) [18] and for [bis(*N*,*N*′-2-*tert*-butylphenylimino)acenaphthene]dibromonickel [14], in opposition to the monomeric structures obtained for other bis(arylimino)acenaphthene nickel complexes, where the nickel centre presents a tetrahedral geometry [14,19]. The Br bridges are unsymmetrical (Ni–Br2 = 2.447(2) and 2.470(2) Å) and somewhat longer than the apical Ni–Br1 bond length of 2.412(2) Å. Compared to the free ligand, the planar geometry of the bis(imino)acenaphtene skeleton is maintained upon coordination to the Ni atom, but the electron delocalization of one of the sides of the ligand precursor is lost, leading to a symmetrical coordinated diimine ligand. As already noted for the free ligand, a small intramolecular N···H–C distance is observed in the complex, whose values (N···H) range from 2.370(9) to 2.433(9) Å.

2.2. Polymerization results

Complex **4** was tested as catalyst precursor for the polymerization of ethylene. The results listed in Table 2 show that diethylaluminium chloride (DEAC) and methylaluminoxane (MAO) are better activators than trimethylaluminium (TMA) or tri-*iso*-butylaluminium (TIBA) for this new α-diimine nickel complex, consistent with other α-diimine nickel complexes [14], [20]. The concentration of **4** (entries LNi3–LNi7) [22], the corresponding [Al]/[Ni] ratio (entries LNi8–LNi12) and the polymerization temperature (entries LNi13–LNi16) seem not to affect significantly the activities of ethylene polymerization. However, the microstructure of PE and consequently their thermal properties are seriously affected by the polymerization temperature (Table 3). It is shown that the polyethylene branching increases with increasing polymerization temperature. Simultaneously, for polymerization runs carried out at room temperature, the total branching of the polymer samples obtained with MAO is smaller than that with DEAC. As can be seen in Table 3, their thermal properties support this conclusion. Actually, the decrease in the polymerization temperature gave more crystalline polymers, with

Table 2
Polymerization of ethylene catalyzed by **4**[a]

Entry	Co-catalyst	[Ni] (μmol l^{-1})	[Al]/[Ni]	Time (min)	Temp (°C)	Yield (g)	Activity[e] × 10^{-7} (g PE (mol Ni [E] h)$^{-1}$)
LNi1	MAO	50	500	7	17	2.239	1.997
LNi2	DEAC	50	250	5.36	17	1.863	2.170
LNi3	DEAC	2.52	720	9.79	19.5	0.610	7.711
LNi4	DEAC	5.04	720	7.95	19.5	0.759	5.906
LNi5	DEAC	10.1	720	6.20	19.5	1.043	5.206
LNi6	DEAC	15.1	720	3.43	19.5	0.700	4.207
LNi7	DEAC	20.2	720	1.31	19.5	0.552	6.495
LNi8	DEAC	5.04	360	5	20.5	0.554	7.010
LNi9	DEAC	5.04	720	4.89	20.5	0.515	6.671
LNi10	DEAC	5.04	1440	5.32	20.5	0.567	6.751
LNi11	DEAC	5.04	1860	5.66	20.5	0.511	5.713
LNi12	DEAC	5.04	2880	6.13	20.5	0.626	6.461
LNi13	DEAC	5.04	720	6.17	0	0.380	3.348
LNi14	DEAC	5.04	720	6.07	20	0.464	4.824
LNi16	DEAC	5.04	720	6.97	60	0.309	4.304
LNi17	TMA	5.04	720	5.90	18	0.124	1.322
LNi18	TIBA	5.04	720	5.74	18	0.128	1.405
LNi19	MAO	5.04	720	6.35	18	0.610	6.058
LNi20	DEAC	5.04	720	7.03	18	0.668	5.989
LNi21	–	5.04	–	35	18	–	–
Ref. [5][b]	MAO	58.6	2100		25		0.257
Ref. [5][c]	MAO	42	3500		25		0.437
Ref. [20][d]	MAO	8.3	2000	60	25		0.207
	DEAC	1.6	500	60	25		0.160

[a] Conditions: toluene (50 ml), P_E = 15 psig.

[b,c] Work performed in our laboratory, using similar conditions of the present work although higher catalyst concentrations; catalysts: [b][NiBr$_2$-(MesBIAN)], [c][NiBr$_2$(*i*PPBIAN)].

[d] Results reported by another group using the catalyst [NiBr$_2$(*i*PPBIAN)].

[e] E concentration determined according to the solubility parameters listed in ASPEN [21]. [E] = 0.3801 M at 17 °C; [E] = 0.3771 M at 18 °C; [E] = 0.3726 M at 19.5 °C; [E] = 0.3711 M at 20 °C; [E] = 0.3696 M at 20.5 °C; [E] = 0.3559 M at 25 °C; [E] = 0.2410 M at 60 °C.

Table 3
Microstructure and thermal properties of selected polyethylene samples

Entry	No. branches/1000 C[a]	ΔH_f (J g^{-1})[b]	T_{onset}[b] (°C)	T_{max}[b,c] (°C)	ΔT[b] (°C)
LNi13 (DEAC, 0 °C)	Traces	182.1 (111.1)	120.1 (109.8)	134.9 (130.1)	~70 (~70)
LNi14 (DEAC, 20 °C)	45	82.5 (71.1[d])	82.1 (22.5[d])	92.9 (80.3[b])	~80[e] (~80)
LNi16 (DEAC, 60 °C)[d]	92	1.5 (–)	33.7 (–)	47.1 (–)	~30 (–)
LNi19 (MAO, 18 °C)	34	108.2 (78.7)	89.5 (71.0)	109.9 (99.0)	~60[f] (~80)

[a] Determined by ^{1}H NMR [24].

[b] Determined by DSC; scans performed from 30 to 200 °C, scan rate: 10 °C/min; values for a second scan between brackets.

[c] The peak value of the melting endotherm (ideally taken as the temperature at which the largest and most perfect crystals are melting) is frequently assigned as the melting temperature, i.e. $T_m \equiv T_{max}$. ΔT values give an approximate idea of the melting range [25].

[d] Scan performed from 15 to 200 °C, scan rate: 10 °C/min.

[e] Two peaks observed.

[f] Shoulder observed.

higher melting temperatures and higher enthalpies of fusion. Sample LNi16 was the only PE soluble in THF at room temperature (GPC data: $M_n = 7.78 \times 10^4$, $M_w/M_n = 1.79$), implying the observed higher extent of branching and/or a lower molecular weight due to a higher polymerization temperature, where chain isomerization and β-hydride elimination reactions are favored.

Complex **4** was also tested for the polymerization of propylene. In this case, a solution of **4** stored at −4 °C for 3 days showed a similar activity to a freshly prepared one, meaning that no decomposition occurred. From Table 4, it is shown that the activity for propylene polymerization is about 10^2 times lower than that of the polymerization of ethylene (compare entry LNi19 with LNi3P). Both the activity and molecular weight increase with the increase of temperature in the range −20–20 °C. However, at 40 °C a decrease, either in the activity or in the M_n, is observed. Thus, the highest activity and the highest molecular weight were obtained at a polymerization temperature of 20 °C. The ^{13}C NMR spectrum of polypropylene (entry LNi5P) shows that atactic PP was obtained [26–28].

Table 4
Polymerization of propylene catalyzed by **4**[a]

Entry	Cocatalyst	[Ni] (μmol l^{-1})	[Al]/[Ni]	T (°C)	Yield (g)	Activity × 10^{-5} (g PP (mol Ni [P]h)$^{-1}$)	$M_n/10^{-4}$	M_w/M_n
LNi5P[b]	DEAC	20.2	720	−20	0.116	0.99	12.9	1.21
LNi2P[b]	DEAC	20.2	720	0	0.280	2.79	13.9	1.52
LNi3P[b]	DEAC	20.2	720	20	0.393	5.66	21.5	1.51
LNi6P[c]	DEAC	50.0	360	−20	0.206	0.66	10.0	1.24
LNi7P[c]	DEAC	50.0	360	0	0.517	2.02	19.8	1.31
LNi8P[c]	DEAC	50.0	360	20	0.700	3.50	16.1	1.73
LNi9P[c]	DEAC	50.0	360	40	0.448	3.18	10.7	1.81

[a] Conditions: toluene (50 ml), P_P = 15.7 psig, 1 h.
[b] Catalyst solution stored in toluene, at −4 °C for 3 days.
[c] Catalyst solution stored in toluene, at −4 °C for 1 day.

The new α-diimine nickel complex, activated by MAO or DEAC, shows much higher activities for ethylene polymerization than those observed in our laboratory for the [bis(*N*,*N*′-dimesitylimino)acenaphthene]-dibromonickel ([$NiBr_2$(MesBIAN)]) and [bis(*N*,*N*′-2, 6-diisopropylphenylimino)acenaphthene]dibromonickel ([$NiBr_2$(*i*PPBIAN)]) [5] in similar conditions except for the catalyst concentrations (see Table 2). It also exhibits higher activities than those shown by other similar Ni catalysts reported either by us [9,14] or other groups [2,18,20], although in some of these studies the experimental conditions are not exactly the same. This difference, observed between the present catalyst and the others, may be partially due to the presence of the electron donor –Si(^{t}Bu)Ph_2 group in the 4-position of the 2,6-dialkylarylimine group. In fact, the activity of these catalysts depends not only on the coordination step (π-complex formed between the metal atom of the catalyst and the double bond of the monomer), but also on the activation energy of the migratory insertion step. The higher the electrophilicity of the metal centre the stronger the σ-bond between the monomer and the metal atom in the π-complex. However, the higher the back-bonding of the metal to the π anti-bonding orbital of the olefin the higher the insertion rate, since a weaker carbon-carbon double bond has to be broken during this step. Thus, the increase of the electron-donor character of the metal atom is expected to increase the insertion rate while the increase of its electrophilicity is expected to increase the strength of the σ-bond of the π-complex. Therefore, both factors must be balanced when predicting the effect of an electron donor substituent on the catalyst activity. In the present case, some theoretical studies (PM3 and DFT) have been performed and preliminary results show that, in fact, the stability of the π-complex is lower than that of the [$NiBr_2$(MesBIAN)] [29]. Studies on the activation energies of the insertion reactions are underway.

It is also found that complex **4** shows higher activity for propylene polymerization than either of the above mentioned α-diimine nickel complexes [2,9,14]. The total number of branches of the polyethylene samples obtained with this new complex **4**, activated either by MAO or DEACis slightly lower than that observed for the polyethylene samples obtained with ([$NiBr_2$(MesBIAN)]) [9]. In fact, while the total number of branches is ca. 3% and 5% when the catalyst systems **4**/MAO and **4**/DEAC are used, it turns to ca. 9% and 10% for the systems [$NiBr_2$(MesBIAN)]/MAO and [$NiBr_2$(MesBIAN)]/DEAC, respectively.

3. Conclusion

A new silylated α-diimine ligand **3** and the corresponding Ni(II) complex **4** have been prepared and characterized. The ligand was modified in an attempt to change the electronic density of the metal center and eventually to improve the activities in either the α-olefin polymerisation or the copolymerisation with polar monomers. The results obtained showed that complex **4**, activated either by diethylaluminum chloride (DEAC) or by methylaluminoxane (MAO), produces highly active catalyst systems for ethylene polymerization and moderately active for propylene polymerization. The higher activities obtained in comparison with the non-silylated α-diimine nickel complexes may be partially attributed to the electron donor effect of the –Si(^{t}Bu)Ph_2 aryl substituent. Investigations on the copolymerization catalysis of the new α-diimine nickel complex are now in progress.

4. Experimental

4.1. General procedures and materials

All manipulations were carried out under an atmosphere of nitrogen using glove box and standard Schlenk techniques, unless stated otherwise. Solvents were predried over activated 4 Å molecular sieves or sodium wire (for toluene) and then distilled under an atmosphere of nitrogen from sodium/benzophenone (diethyl ether and tetrahydrofuran), sodium/potassium alloy (toluene) or calcium hydride (methanol, dichloromethane and *n*-hexane), and stored under nitrogen. Deuterated solvents (C_6D_6, CD_2Cl_2 and $CDCl_3$) for NMR samples were dried with activated 4 Å molecular sieves, degassed by freeze-pump-thaw cycles and stored in ampoules over activated 4 Å molecular sieves.

The NMR spectra were recorded on a Varian Unity 300 (^1H, 300 MHz; ^{13}C, 75.43 MHz) spectrometer and referenced internally using residual proton- (^1H) and carbon-(^{13}C) solvent resonances relative to tetramethylsilane (TMS, $\delta = 0$ ppm). NMR analyses of the polyethylenes were performed on samples dissolved in a mixture of 1,2,4-trichlorobenzene/C_6D_6 (v/v = 1:1) at 110 °C, and the internal reference was provided by hexamethyldisiloxane (δ^1H 0.058, $\delta^{13}C$ 1.9 relative to TMS). Polypropylene NMR analyses were performed on samples dissolved in $CDCl_3$ at 50 °C and referenced to internal TMS. Elemental analyses were performed on a Fisons Instrument Mod EA-1108 analyzer by the Laboratório de Análises in this Institute. Differential Scanning Calorimetry (DSC) analyses of the polymers were performed on a Setaram DSC121 calorimeter. In order to minimize the differences in the thermal history of the samples, the polymers were subjected to heating/cooling/heating cycles under argon, between 15 or 20 °C and 200 °C using heating and cooling rates of 10 °C/min. After the first heating scan, the samples remained at 200 °C for 10 min. The results obtained in the first and second heating runs were registered and are presented. During the experiments the sample holder was continuously purged with argon. Molecular weight measurements were performed by Gel Permeation Chromatography/Size Exclusion Chromatography (GPC/SEC) on a Waters 150 CV chromatograph at 30 °C. A series of three columns Waters Ultrastyragel HR-1, HR-3 and HR-4 (10 μm; 30 × 0.8 cm) were used, and the eluant was THF at a flow rate of 1 cm^3 min^{-1}. The calibration was made using polystyrene standards (TSK Tosoh Co.).

Reagents as 2,6-isopropylaniline, *tert*-butyllithium, *tert*-butyldiphenylsilyl chloride, diethylaluminium chloride, trimethylaluminium, tri-*iso*-butylaluminium (Aldrich Chemical Company), acenaphthenoquinone, bromine, formic acid, concentrated hydrochloric acid, anhydrous $NiBr_2$ (Acros Organics), glacial acetic acid (Merck) and methylaluminoxane (Akzo Chemical Company) were purchased and used as received. [$NiBr_2$(DME)] (DME = dimethoxyethane) was prepared according to the literature [30].

4.2. Synthesis of 2,6-diisopropyl-aniline hydrochloride

Under air atmosphere, concentrated hydrochloric acid (50 ml, excess) was added dropwise to 2,6-isopropylaniline (50 ml, 0.265 mol) dispersed in water (250 ml). The reaction mixture was further stirred for 1 h after the addition was completed. The resulting white precipitate was collected and washed with water, then dried in a vacuum oven at room temperature to give the desired product in 87% yield.

4.3. Synthesis of compound 4-bromo-2,6-diisopropyl-aniline (*1*)

Compound **1** was obtained by modification of a reported procedure [13,31]. Br_2 (8.64 ml, 0.168 mol) was added via a dropping funnel to a stirred solution of 2,6-isopropylaniline hydrochloride (35.9 g, 0.168 mol) in methanol (100 ml) and glacial acetic acid (50 ml). The resulting mixture was further stirred for 2 h. The precipitated salt ([4-Br–C_6H_4–NH_3][Cl]) was filtered and washed with fresh acetic acid, air dried and recrystallized from hot benzene. The free base was prepared by adding aqueous NaOH and diethyl ether to the solid salt. The ether phase was dried over $MgSO_4$, filtered, and the diethyl ether removed via rotary-evaporation to yield a crude brown liquid product. At last, purified by trap-to-trap distillation, colorless **1** was obtained in 79% yield. ^1H NMR (300 MHz; CD_2Cl_2): δ_H 1.22 (12H, d, CH_3, $^3J_{HH} = 6.9$ Hz), 2.86 (2H, hept, CH, $^3J_{HH} = 6.9$ Hz), 3.75 (2H, br, NH_2), 7.09 (2H, s, ArH).

4.4. Synthesis of compound 2,6-diisopropyl-4-tert-butyldiphenylsilyl-aniline (*2*)

To a stirred solution of **1** (14.52 g, 56.7 mmol) in THF (180 ml) at −70 °C was slowly added dropwise of a 1.7 mol dm^{-3} solution of *tert*-butyllithium in pentane (100 ml, 0.17 mol). The solution was stirred overnight and let warm up to room temperature. Then a solution of *tert*-butyldiphenylsilyl chloride (14.7 ml, 56.7 mmol) in THF (80 ml) was added dropwise via cannula at −20 °C. The mixture was stirred overnight at room temperature and hydrolyzed with 500 ml of aqueous saturated NH_4Cl. The organic phase was separated, and the aqueous layer was extracted twice with $CHCl_3$. The combined organic phases were dried over $MgSO_4$ and filtered, and the solvent removed. The residue was purified in a chromatography column ($L = 40$ cm) eluted by hexane/diethyl ether (v/v = 6:1) to give white needle crystals of **2** in 25% yield. ^1H NMR (300 MHz; CD_2Cl_2): δ_H 1.14 (9H, s, CH_3), 1.16 (12H, d, CH_3, $^3J_{HH} = 6.9$ Hz), 2.89 (2H, hept, CH, $^3J_{HH} = 6.9$ Hz), 3.88 (2H, br, NH_2), 7.19 (2H, s, ArH), 7.3–7.6 (10H, m, ArH).

4.5. Synthesis of ligand bis[N,N′-(4-tert-butyl-diphenylsilyl-2,6-diisopropylphenyl)imino]acenaphthene (*3*)

Acenaphthenequinone (0.25 g, 1.37 mmol), methanol (50 ml) and a slight excess of compound **2** (1.25 g, 3.01 mmol) were placed in a 100 ml flask and allowed to stir for 3 days in the presence of a formic acid (a few drops). CH_2Cl_2 and water were added and the layers were separated. The resulting organic layer was dried with $MgSO_4$, filtered and the solvent was removed to give the crude new ligand as an orange solid. The impure ligand was recrystallized from hot toluene to give orange crystals of **3** in 64% yield. ^1H NMR (300 MHz; CD_2Cl_2): δ_H 0.90 (12H, s, CH_3), 1.15 (12H, d, CH_3, $^3J_{HH} = 5.4$ Hz), 1.25 (18H, s, CH_3), 2.94 (4H, hept, CH, $^3J_{HH} = 5.4$ Hz), 6.64 (2H, s, ArH), 7.1–7.9 (28H, m, ArH). Anal. Calc. for $C_{68}H_{76}N_2Si_2$: C, 83.55; H, 7.84; N, 2.87. Found: C, 83.80; H, 8.40; N, 2.90%.

4.6. Synthesis of complex bis[N,N′-(4-tert-butyldiphenylsilyl-2,6-diisopropylphenyl)imino]acenaphthene (4)

Complex **4** was prepared using two procedures:

(a) Acenaphthenequinone (0.5 g, 2.75 mmol) and a slight excess of compound **2** (2.5 g, 6.04 mmol) were placed in a Schlenk tube followed by 100 ml glacial acetic acid, forming a brown-red solution within minutes. This mixture was heated to reflux for 4 h. Anhydrous $NiBr_2$ (0.61 g, 2.75 mmol) was added as a solid to this mixture and the reaction was allowed to reflux overnight. The solvent was removed in vacuum and the resulting solid was washed with diethyl ether (20 ml × 3). The residue was extracted with CH_2Cl_2 and the resulting deep red solution was filtered via a cannula to another Schlenk tube. This procedure was repeated twice and the solvent was removed in vacuum to give a dark brown-red powder **4** in 61% yield, that is suitable for elemental anlaysis and polymerization use. Crystals of complex **4** suitable for X-ray studies were obtained by dissolving a small amount of **4** in CH_2Cl_2 double-layered with hexane. The mixture was allowed to sit undisturbed overnight. The resulting red crystals formed at the sides of the tube and the filtrate was decanted. The crystals were used immediately for X-ray and elemental analysis. Anal. Calc. for $C_{68}H_{76}Br_2N_2NiSi_2 \cdot 0.25CH_2Cl_2$: C, 67.34; H, 6.33; N, 2.30. Found: C, 67.36; H, 6.71; N, 2.35%.

(b) $[NiBr_2(DME)]$ (0.27 g, 0.88 mmol), the ligand **3** (0.85 g, 0.87 mmol) and CH_2Cl_2 (50 ml) were combined in a Schlenk tube and stirred at room temperature for 16 h. The resulting suspension was filtered and the solvent of the filtrate removed under vacuum. The resulting solid was washed with Et_2O (20 ml × 3) to give brown-red complex **4** in 87% yield.

4.7. Polymerization procedure

Polymerizations of ethylene and propylene were carried out in a flame dried 250 ml crown capped pressure bottle sealed with neoprene septum and pump filled with nitrogen atmosphere. To this polymerization bottle

Table 5
Crystal data, data collection and refinement parameters for **3** and **4**

Compound	**3**	**4**
Empirical formula	$C_{68}H_{76}N_2Si_2$	$C_{68}H_{76}Br_2N_2NiSi_2$
Formula weight	977.49	1196.02
Crystal color	Orange	Red
Crystal size (mm)	0.5 × 0.1 × 0.08	0.50 × 0.45 × 0.15
Crystal system	Monoclinic	Monoclinic
Space group	$P2_1$	$P2_1/n$
a (Å)	8.794(4)	14.669(4)
b (Å)	30.428(8)	31.549(8)
c (Å)	11.545(4)	14.939(4)
β (°)	100.98(2)	115.45(2)
V (Å^3)	3033(2)	6243(3)
Z	2	4
D_{calc} (g cm^{-3})	1.070	1.273
μ (mm^{-1})	0.821	1.670
$F(000)$	1052	2496
θ range (°)	4.16–66.98	1.63–24.95
Limiting indices	$0 \leqslant h \leqslant 10$; $-31 \leqslant k \leqslant 0$; $-13 \leqslant l \leqslant 13$	$-17 \leqslant h \leqslant 0$; $-37 \leqslant k \leqslant 0$; $-15 \leqslant l \leqslant 17$
Completeness to θ (%)	94.4	98.2
Reflections collected	5566	11353
Unique data [$I > 2\sigma(I)$]	5214 ($R_{int} = 0.0128$)	10904 ($R_{int} = 0.1390$)
Goodness of fit	1.049	0.815
Refined parameters	645	676
R_1 [$I > 2\sigma(I)$]	0.0626	0.0935
wR_2 [$I > 2\sigma(I)$]	0.1624	0.0798
R_1,wR_2 all data	0.0761/0.1712	0.3407/0.1134
Abs. struct. parameter	−0.04(6)	–
Larg. peak/hole (e Å^{-3})	0.593 and −0.325	0.433 and −0.619

50 ml of dry toluene were added and the resulting solvent was then saturated at a monomer relative pressure of 1 bar, which was maintained throughout the polymerization reactions. Then, the co-catalyst was added in the proper Al/Ni ratio via a glass syringe. At this time, the solutions were brought to the desired temperatures and allowed to equilibrate for 15 min. After this, the corresponding amount of a toluene solution of the Ni catalyst was added to the polymerization reactors. The polymerizations were terminated after several minutes for ethylene and 1 h for propylene by quenching the mixture with 150 ml of a 2% HCl/methanol solution. The obtained polymers were then filtered, washed several times with 50 ml portions of methanol and dried in a vacuum oven at 50 °C for 3 days.

4.8. X-ray crystallography

Crystal structures were obtained using a MACH3 Nonius diffractometer equipped with Mo radiation ($\lambda = 0.71069$ Å) for complex **4** and a TURBO CAD4 with a Cu rotating anode ($\lambda = 1.54180$ Å) in compound **3**. All data were corrected for Lorentz, polarization and long term intensity fluctuations. Absorption effects in complex **4** were corrected using DIFABS [32]. Structures were solved by direct methods using SIR97 [33] and refined by full-matrix least squares against F^2 using SHELXL [34], all included in the suite of programs WINGX v1.64.05 for Windows [35]. ORTEP III [36] diagrams with selected atomic labeling are presented in Figs. 1 and 2.

In both structures all non-hydrogen atoms were refined anisotropically and the hydrogen atoms were inserted in idealized positions riding in the parent C atom.

Details of data collection and crystal refinement for **3** and **4** are summarized in Table 5. As can be seen, the crystal of complex **4** was found to diffract very poorly.

5. Supplementary material

Crystallographic data for the structural analyses have been deposited with the Cambridge Crystallographic Data Centre, CCDC, Nos. 239956 and 239957 for the ligand **3** and the complex **4**, respectively. Copies of this information may be obtained free of charge from: The Director, CCDC, 12 Union Road, Cambridge CB2 1EZ UK (Fax: +44-1223-336033; E-mail: deposit@ccdc.cam.ac.uk or www: http://ccdc.cam.ac.uk).

Acknowledgements

This work was funded by Fundação Luso-Americana para o Desenvolvimento (Projet 122/2000), Fundação para a Ciência e Tecnologia (Projects POCTI/QUI/32771/99 and POCTI/QUI/42015/2001 and Grants SFRH/BPD/3522/2000 and PRAXIS XXI/BD/19638/99, respectively, to H-R.L. and to S.I.C.), FSE and FEDER. We are grateful to DST, India, and GRICES, Portugal, for grants under Indo-Portuguese Collaboration for this investigation. We appreciate the support by Borealis in the polymerization equipment.

References and Notes

[1] S.D. Ittel, L.K. Johnson, M. Brookhart, Chem. Rev. 100 (2000) 1169–1203.

[2] L.K. Johnson, C.M. Killian, M. Brookhart, J. Am. Chem. Soc. 117 (1995) 6414–6415.

[3] C.M. Killian, D.J. Tempel, L.K. Johnson, M. Brookhart, J. Am. Chem. Soc. 118 (1996) 11664–11665.

[4] L.K. Johnson, S. Mecking, M. Brookhart, J. Am. Chem. Soc. 118 (1996) 267–268.

[5] S.G. Correia, M.M. Marques, J.R. Ascenso, A.F.G. Ribeiro, P.T. Gomes, A.R. Dias, M. Blais, M.D. Rausch, J.C.W. Chien, J. Polym. Sci. Part A: Polym. Chem. 37 (1999) 2471–2480.

[6] M.M. Marques, S. Fernandes, S.G. Correia, J.R. Ascenso, S. Caroço, P.T. Gomes, J. Mano, S.G. Pereira, T. Nunes, A.R. Dias, M.D. Rausch, J.C.W. Chien, Macromol. Chem. Phys. 201 (2000) 2464–2468.

[7] S. Fernandes, M.M. Marques, S.G. Correia, J. Mano, J.C.W. Chien, Macromol. Chem. Phys. 201 (2000) 2566–2572.

[8] M.M. Marques, S. Fernandes, S.G. Correia, S. Caroço, P.T. Gomes, A.R. Dias, J. Mano, M.D. Rausch, J.C.W. Chien, Polym. Int. 50 (2001) 579–587.

[9] J.C.W. Chien, S. Fernandes, S.G. Correia, M.D. Rausch, L.C. Dickson, M.M. Marques, Polym. Int. 51 (2002) 729–737.

[10] L. Wang, E. Hauptman, L. Johnson, E. McCord, Y. Wang, S.D. Ittel, World Pat, WO 01/92342 A2 (DuPont), 2001.

[11] L. Johnson, L. Wang, S. McLain, A. Bennett, K. Dobbs, E. Hauptman, A. Ionkin, S. Ittel, K. Kunitsky, W. Marshall, E. McCord, C. Radzewich, A. Rinehart, K.J. Sweetman, Y. Wang, Z. Yin, M. Brookhart, ACS Sym. Ser. 857 (2003) 131–142.

[12] G. van koten, K. Vrieze, Adv. Organomet. Chem. 21 (1982) 151–239.

[13] J.H. Oskam, H.H. Fox, K.B. Yap, D.H. McConville, R. O'Dell, B.J. Lichtenstein, R.R. Schrock, J. Organomet. Chem. 459 (1993) 185–198.

[14] R.J. Maldanis, J.S. Wood, A. Chandrasekaran, M.D. Rausch, J.C.W. Chien, J. Organomet. Chem. 645 (2002) 158–167.

[15] H. Allen, CCDC/CSD, Acta Cryst. B, 58 (2002) 380–388.

[16] U. El-Ayaan, A. Paulovicova, Y. Fukuda, J. Mol. Struct. 645 (2003) 205–212.

[17] R. van Asselt, C.J. Elsevier, W.J.J. Smeets, A.L. Spek, R. Benedix, Recl. Trav. Chim. Pays-Bas 113 (1994) 88–98.

[18] J.O. Liimatta, B. Lofgren, M. Miettinen, M. Ahlgren, M. Haukka, T.T. Pakkanen, J. Polym. Sci. Part A: Polym. Chem. 39 (2001) 1426–1434.

[19] D.P. Gates, S.A. Svejda, E. Oñate, C.M. Killian, L.K. Johnson, P.S. White, M. Brookhart, Macromolecules 33 (2000) 2320–2334.

[20] K.R. Kumar, S. Sivaram, Macromol. Chem. Phys. 201 (2000) 1513.

[21] AspenTech, Aspen Engineering Suite^{TM} 10.2.

[22] In entries LNi3–LNi7 different polymerization times were used sometimes slightly higher and sometimes slightly lower than those used in the other runs reported (usually around 6/7 min). This occurred because either a very high concentration of polymer in the solution inside the reactor or a very low one was expected for higher or lower catalyst concentrations in the feed, respectively.

These are undesired situations since, in the first case, mass transport limitations could occur and, in the second case, a very low amount of polymer could be obtained. However, the kinetic studies underway [23] show that the kinetic profiles are not of a decay type and an almost constant polymerization rate along the time is observed. Besides, the results obtained show that the values of the activity observed in the range of catalyst concentrations studied are very similar and no particular trend could be observed. Thus the effect of the polymerization time in the activity, if any, can be neglected.

[23] I. Matos; F. Lemos, M.M. Marques, unpublished work.
[24] A.C. Gottfried, M. Brookhart, Macromolecules 36 (2003) 3085–3100.
[25] R.P. Chartoff, in: E.A. Turi (Ed.), Thermal Characterization of Polymeric Materials, Academic Press, San Diego, USA, 2003.
[26] H.N. Cheng, D.A. Smith, Macromolecules 19 (1986) 2065–2072.
[27] A. Grassi, A. Zambelli, L. Resconi, E. Albizzati, R. Mazzocchi, Macromolecules 21 (1988) 617–622.
[28] V. Busico, R. Cipullo, P. Corradini, L. Landriani, M. Vacatello, A.L. Segre, Macromolecules 28 (1995) 1887–1892.
[29] M.A.N.D.A. Lemos, F. Lemos, M.M. Marques, unpublished work.
[30] L.G.L. Ward, Inorg. Synth. 13 (1972) 154–164.
[31] R.A. Benkeser, R.A. Hickner, D.I. Hoke, O.H. Thomas, J. Am. Chem. Soc. 80 (1958) 5289–5294.
[32] N. Walker, D. Stuart, DIFABS, Acta Cryst. A 39 (1983) 158–166.
[33] A. Altomare, M.C. Burla, M. Camalli, G. Cascarano, C. Giacovazzo, A. Guagliardi, A.G.G. Moliterni, G. Polidori, R. Spagna, J. Appl. Cryst. 32 (1999) 115–119.
[34] G.M. Sheldrick, SHELXL-97: A Computer Program for Refinement of Crystal Structures, University of Göttingen, 1997.
[35] L.J. Farrugia, WINGX (v1.64.03b), J. Appl. Cryst. 32 (1999) 837–838.
[36] J. Farrugia, ORTEP-3 for Windows (v1.076), based on ORTEP-III (v1.0.3) by C.K. Johnson, M.N. Burnett, J. Appl. Cryst. 30 (1997) 565.